

# Bisubstrate Inhibitor Approach for Targeting Mitotic Kinase Haspin

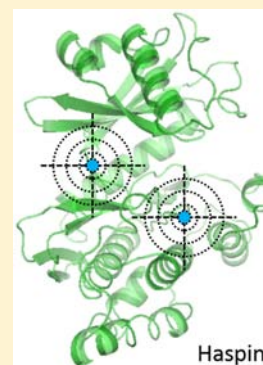
Katrin Kestav,<sup>†</sup> Darja Lavogina,<sup>†</sup> Gerda Raidaru,<sup>†</sup> Apirat Chaikuad,<sup>‡</sup> Stefan Knapp,<sup>\*,‡</sup> and Asko Uri<sup>\*,†</sup>

<sup>†</sup>University of Tartu, Institute of Chemistry, Ravila 14A, Tartu 50411, Estonia

<sup>‡</sup>University of Oxford, Nuffield Department of Clinical Medicine, Structural Genomics Consortium, Old Road Campus Research Building, Oxford OX3 7DQ, United Kingdom

**S** Supporting Information

**ABSTRACT:** During the past decade, the basophilic atypical kinase Haspin has emerged as a key player in mitosis responsible for phosphorylation of Thr3 residue of histone H3. Here, we report the construction of conjugates comprising an aromatic fragment targeted to the ATP-site of Haspin and a peptide mimicking the N-terminus of histone H3. The combination of effective solid phase synthesis procedures and a high throughput binding/displacement assay with fluorescence anisotropy readout afforded the development of inhibitors with remarkable subnanomolar affinity toward Haspin. The selectivity profiles of novel conjugates were established by affinity studies with a model basophilic kinase (catalytic subunit of cAMP-dependent protein kinase) and by a commercial 1-point inhibition assay with 43 protein kinases.



## INTRODUCTION

Haspin kinase (GSG2) is a basophilic Ser/Thr protein kinase (PK) that belongs to the group of atypical PKs.<sup>1</sup> Due to remarkable differences in its catalytic domain as compared to the “canonical kinases” (e.g., His651 is substituted in Haspin for the “classical” catalytically important Lys responsible for chelation of ATP phosphate groups),<sup>2,3</sup> Haspin was initially considered to be an inactive pseudokinase. Recently, however, it has been demonstrated that Haspin is catalytically active and serves as an important player in mitosis.<sup>4–6</sup>

The only well-established physiological substrate of Haspin is histone H3 which is phosphorylated by Haspin at Thr3 creating a docking site for Survivin, which can then coordinate mitotic processes as a part of the chromosomal passenger complex also involving Borealin, INCENP, and protein kinase Aurora B.<sup>7–10</sup> The cocrystal structure of Haspin with histone H3(1–7) peptide revealed a unique binding mode of the substrate peptide with U-shaped turn of the backbone allowing the formation of interactions with both the N- and C-lobes of Haspin.<sup>11</sup> Such an unusual conformation of the bound substrate peptide suggests that Haspin-selective compounds can be generated serving as inhibitors and/or optical probes of Haspin by targeting its substrate site.

So far, only two highly potent inhibitors of Haspin have been disclosed, 5-iodotubercidin and LDN-192960 (Figure 1).<sup>10,12,13</sup> Both compounds target the ATP-site of Haspin, and do not utilize the unique structural and conformational features of the catalytic core of this PK. Also, the labeling of 5-iodotubercidin without the loss of its affinity is synthetically challenging (our unpublished data), and no fluorescent probes for Haspin have so far been reported. The latter tools could potentially aid both

working out of quick biochemical assays as well as research of Haspin-related pathways in mitosis.

In this study, we set out to develop a novel class of Haspin-targeting scaffolds representing the bisubstrate-analogue inhibitors of PKs. Bisubstrate inhibitors comprise a fragment (nucleoside mimic) binding to the ATP-site of a PK and a fragment (peptide) binding to the protein substrate-site of a PK; these fragments are joined by a linker chain (Figure 1).<sup>14</sup> The adenosine analogue–oligoarginine conjugates developed in our research group (generally termed ARCs) are “assembled” using highly efficient and flexible solid phase synthesis procedures, enabling easy modification strategies and parallel syntheses of several compounds. The bisubstrate-analogue nature of such conjugates (as compared to the affinities of individual fragments) ideally translates into their increased affinity as well as improved selectivity toward basophilic PKs (i.e., those phosphorylating preferably substrates that incorporate positively charged amino acid residues in the proximity of the phosphorylation site).<sup>15–17</sup> So far, the selectivity of the previously reported ARCs toward their biological targets was mainly achieved by incorporation of selective nucleoside-mimicking fragments and/or variation of the linkers or chiral spacers, whereas the oligoarginine peptide had mostly served as a generic fragment responsible for recognition of basophilic PKs and as an entity promoting internalization of the conjugates into live cells.<sup>16–18</sup>

Here, we aimed at incorporation of histone H3(1–7) peptide in the structure of conjugates as the fragment targeting the

**Received:** October 10, 2014

**Revised:** January 1, 2015

**Published:** January 16, 2015

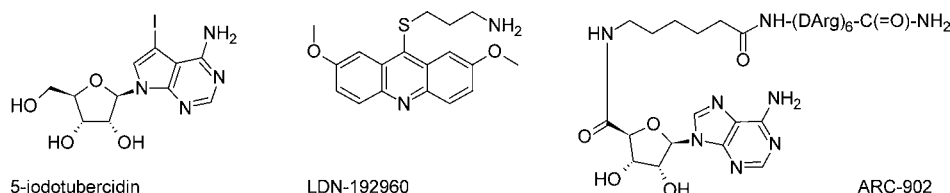


**Figure 1.** Structures of commercially available Haspin inhibitors (5-iodotubercidin, LDN-192960) and the lead compound used in this study (ARC-902).

**Table 1.** Values of the Dissociation Constant  $K_D$  Established in the Binding Assay by Titration with Haspin

compound	schematic structure	$K_D$ , nM <sup>a</sup>
ARC-583	Adc-Ahx-DArg <sub>6</sub> -DLys <sup>b</sup> (TAMRA)-NH <sub>2</sub>	2.0 (0.8)
ARC-669	AMTH-Ahx-DArg-Ahx-DArg <sub>6</sub> -DLys <sup>b</sup> (TAMRA)-NH <sub>2</sub>	9.2 (2.5)
ARC-1042	Adc-Ahx-DArg-Ahx-DArg <sub>6</sub> -DLys <sup>b</sup> (TAMRA)-NH <sub>2</sub>	0.91 (0.28)
ARC-1059	H9-(CH <sub>2</sub> ) <sub>5</sub> -C(=O)-DArg <sub>6</sub> -DLys <sup>b</sup> (TAMRA)-NH <sub>2</sub>	2.0 (0.3)
ARC-1081	Adc-Ahx-DArg-Ahx-DArg <sub>6</sub> -DLys <sup>b</sup> (Cy3B)-NH <sub>2</sub>	1.0 (0.2)
ARC-1144	AMSE-Ahx-DArg-Ahx-DArg <sub>6</sub> -DLys <sup>b</sup> (TAMRA)-NH <sub>2</sub>	23 (8)

<sup>a</sup>Standard error values are given in brackets ( $N = 2$  or more). <sup>b</sup>Points to the DLys residue whose side-chain amino group was used for the attachment of the fluorescent dye.

**Table 2.** Values of the Dissociation Constant  $K_D$  of Nonfluorescent Compounds Established in the Displacement Assay with Haspin and Fluorescent Probe ARC-1081<sup>a</sup>

compound	schematic structure	$K_D$ , nM <sup>b</sup>
ARC-1010	Adc-Ahx	over 15000
ARC-1034	Adc-Ahx-DArg <sub>2</sub> -NH <sub>2</sub>	3400 (400)
ARC-582	Adc-Ahx-DArg <sub>4</sub> -NH <sub>2</sub>	110 (8)
ARC-902	Adc-Ahx-DArg <sub>6</sub> -NH <sub>2</sub>	2.6 (0.3)
ARC-1090	Adc-Ahx-DArg <sub>8</sub> -NH <sub>2</sub>	9.0 (1.1)
ARC-341	Adc-Ahx-LArg <sub>6</sub> -NH <sub>2</sub>	40 (4)
ARC-342	Adc-Ahx-LArg <sub>6</sub> -Lys-NH <sub>2</sub>	33 (2)
ARC-1012	Adc-Ahx-DLys-Ahx-DArg <sub>2</sub> -NH <sub>2</sub>	2000 (200)
ARC-1038	Adc-Ahx-Lys-Ahx-DArg <sub>2</sub> -NH <sub>2</sub>	2000 (100)
ARC-1041	Adc-Ahx-DArg-Ahx-DArg <sub>6</sub> -DLys-NH <sub>2</sub>	0.24 (0.11)
ARC-1176	AMTH-Ahx-DArg-NH <sub>2</sub>	over 15000
ARC-1102	AMTH-Ahx-DLys-Ahx-DArg <sub>2</sub> -NH <sub>2</sub>	over 15000
ARC-668	AMTH-Ahx-DArg-Ahx-DArg <sub>6</sub> -DLys-NH <sub>2</sub>	15 (3)
ARC-1141	AMTH-Ahx-DAla-DArg <sub>6</sub> -DLys-Gly	16 (3)
ARC-1143	AMTH-Ahx-DAla-DArg <sub>6</sub> -DLys <sup>c</sup> (Myr)-Gly	66 (5)
ARC-1197	AMTH-Ahx-DArg-Ahx-DArg <sub>6</sub> -DLys <sup>c</sup> (-C(=O)-(CH <sub>2</sub> ) <sub>7</sub> -C(=O)-DArg <sub>6</sub> -NH <sub>2</sub> )-NH <sub>2</sub>	4.7 (0.5)
ARC-3009	H9-C(=O)-CH <sub>2</sub> -NH-CH <sub>2</sub> -C(=O)-DArg <sub>2</sub> -NH <sub>2</sub>	over 15000
ARC-3010	H9-C(=O)-CH <sub>2</sub> -NH-CH <sub>2</sub> -C(=O)-DArg <sub>6</sub> -NH <sub>2</sub>	800 (160)
ARC-903	H9-(CH <sub>2</sub> ) <sub>5</sub> -C(=O)-DArg <sub>6</sub> -NH <sub>2</sub>	37 (3)
ARC-1408	PIPY-C(=O)-(CH <sub>2</sub> ) <sub>7</sub> -C(=O)-DArg-Ahx-DArg-NH <sub>2</sub>	3700 (600)
ARC-1411	PIPY-C(=O)-(CH <sub>2</sub> ) <sub>7</sub> -C(=O)-DArg <sub>6</sub> -DLys-NH <sub>2</sub>	11 (2)
ARC-684	PYB-Ahx-DArg-Ahx-DArg <sub>6</sub> -DLys-NH <sub>2</sub>	17 (3)
ARC-685	PYB-Ahx-DArg-Ahx-DArg <sub>6</sub> -DLys <sup>c</sup> (Myr)-NH <sub>2</sub>	390 (50)
ARC-3125	TIBI-CH <sub>2</sub> -C(=O)-Ahx-DArg <sub>6</sub> -DLys-NH <sub>2</sub>	0.56 (0.09)
-	DArg <sub>9</sub> -NH <sub>2</sub>	over 15000

<sup>a</sup>Compounds are listed in alphabetical order according to their ATP-site binding fragments. <sup>b</sup>Standard error values are given in brackets ( $N = 2$  or more). <sup>c</sup>Points to the DLys residue whose side-chain amino group was used for the attachment of the fragment in brackets.

protein substrate-site of Haspin and conferring selectivity of novel conjugates to this target. For that, we first established a quick and reliable binding/displacement assay with fluorescence polarization/anisotropy readout, and used it for screening of a large set of previously reported ARCs that had been used for targeting basophilic PKs. Next, we established the possible ways to link the nucleoside mimics to the histone H3(1–7) peptide and performed the synthesis of several new ARCs. The affinity of the conjugates toward Haspin and a reference

basophilic kinase was established in the binding/displacement assay, and two novel compounds were profiled toward a panel of 43 PKs for wider selectivity studies.

## RESULTS AND DISCUSSION

**Binding/Displacement Assay Using Previously Reported ARC-Scaffolds.** We started the study by choosing a set of structurally diverse fluorescent ARC-based probes to be screened toward Haspin in a biochemical binding assay<sup>19</sup>

Table 3. Values of the Thermal Shift  $\Delta T_m$  of Nonfluorescent Compounds with Haspin, CLK1, CLK2, and DYRK2<sup>a</sup>

compound	schematic structure	$\Delta T_m$ , °C <sup>b</sup> Haspin	$\Delta T_m$ , °C <sup>b</sup> CLK1	$\Delta T_m$ , °C <sup>b</sup> CLK2	$\Delta T_m$ , °C <sup>b</sup> DYRK2
ARC-1034	Adc-Ahx-DArg <sub>2</sub> -NH <sub>2</sub>	4.5 (0.1)	2.5 (0.2)	0.6 (0.1)	1.2 (0.0)
ARC-902	Adc-Ahx-DArg <sub>6</sub> -NH <sub>2</sub>	<b>8.6 (0.2)</b>	3.4 (0.1)	1.0 (0.1)	0.8 (0.0)
ARC-341	Adc-Ahx-LArg <sub>6</sub> -NH <sub>2</sub>	<b>5.7 (0.1)</b>	2.5 (0.2)	0.8 (0.0)	0.6 (0.0)
ARC-1012	Adc-Ahx-DLys-Ahx-DArg <sub>2</sub> -NH <sub>2</sub>	4.6 (0.1)	1.4 (0.1)	0.7 (0.1)	1.9 (0.0)
ARC-1038	Adc-Ahx-Lys-Ahx-DArg <sub>2</sub> -NH <sub>2</sub>	4.2 (0.1)	0.8 (0.0)	0.3 (0.1)	0.4 (0.0)
ARC-1102	AMTH-Ahx-DLys-Ahx-DArg <sub>2</sub> -NH <sub>2</sub>	2.8 (0.0)	3.2 (0.1)	1.9 (0.0)	2.8 (0.0)
ARC-668	AMTH-Ahx-DArg-Ahx-DArg <sub>6</sub> -DLys-NH <sub>2</sub>	<b>8.0 (0.1)</b>	<b>5.6 (0.0)</b>	3.9 (0.1)	2.1 (0.0)
ARC-1141	AMTH-Ahx-DAla-DArg <sub>6</sub> -DLys-Gly	<b>6.0 (0.1)</b>	<b>5.3 (0.1)</b>	3.1 (0.1)	2.2 (0.1)
ARC-3009	H9-C(=O)-CH <sub>2</sub> -NH-CH <sub>2</sub> -C(=O)-DArg <sub>2</sub> -NH <sub>2</sub>	1.1 (0.1)	1.2 (0.1)	0.3 (0.1)	0.3 (0.1)
ARC-3010	H9-C(=O)-CH <sub>2</sub> -NH-CH <sub>2</sub> -C(=O)-DArg <sub>6</sub> -NH <sub>2</sub>	2.0 (0.1)	0.7 (0.0)	0.3 (0.1)	0.2 (0.0)
ARC-1408	PIPY-C(=O)-(CH <sub>2</sub> ) <sub>7</sub> -C(=O)-DArg-Ahx-DArg-NH <sub>2</sub>	3.9 (0.0)	4.8 (0.5)	3.2 (0.0)	2.0 (0.1)
ARC-1411	PIPY-C(=O)-(CH <sub>2</sub> ) <sub>7</sub> -C(=O)-DArg <sub>6</sub> -DLys-NH <sub>2</sub>	<b>7.8 (0.1)</b>	<b>5.8 (0.3)</b>	3.9 (0.1)	1.1 (0.0)
ARC-684	PYB-Ahx-DArg-Ahx-DArg <sub>6</sub> -DLys-NH <sub>2</sub>	<b>5.7 (0.1)</b>	−1.8 (0.2)	0.6 (0.0)	−1.1 (0.0)
ARC-685	PYB-Ahx-DArg-Ahx-DArg <sub>6</sub> -DLys <sup>c</sup> (Myr)-NH <sub>2</sub>	2.8 (0.1)	2.0 (0.2)	−5.2 (0.4)	0.4 (0.0)
ARC-3125	TIBI-CH <sub>2</sub> -C(=O)-Ahx-DArg <sub>6</sub> -DLys-NH <sub>2</sub>	<b>10.1 (0.1)</b>	<b>6.5 (0.2)</b>	4.0 (0.1)	3.3 (0.0)

<sup>a</sup>Compounds are listed in alphabetical order according to their ATP-site binding fragments. <sup>b</sup>Standard error values are given in brackets ( $N = 2$  or more).  $\Delta T_m$  values of over 5 °C are shown in bold. <sup>c</sup>Points to the DLys residue whose side-chain amino group was used for the attachment of the fragment in brackets.

(detailed structures of the probes are given in Supporting Information Table S1). The initially chosen ARCs had previously revealed low nanomolar or subnanomolar dissociation constants ( $K_D$  values) toward their reported PK targets (cAMP- and cGMP-dependent PKs, Rho kinase, etc.) and relatively broad selectivity profiles according to studies in commercial PK panels.<sup>17,19–22</sup>

According to the results of the titration of the probes with Haspin protein (summarized in Table 1 and Supporting Information Table S2), the lowest  $K_D$  values (0.9 nM and 1 nM, respectively) were established for conjugates ARC-1042 and ARC-1081. Both compounds incorporated adenosine-4'-dehydroxymethyl-4'-carboxylic acid moiety (Adc) as the PK ATP-site targeting fragment and (DArg)<sub>6</sub>-DLys as the PK protein substrate-site targeting fragment linked by two flexible 6-aminohexanoic acid moieties (Ahx) and a chiral DArg spacer; fluorescent dyes (TAMRA or Cy3B, respectively) were attached to the C-termini of conjugates via the side-chain of DLys residue.

Next, displacement of the probe ARC-1081 from its complex with Haspin was performed by a larger set of nonfluorescent ARCs representing variable structural scaffolds to identify inhibitors that could serve as starting points (lead compounds) for the design of Haspin-selective inhibitors (detailed structures of compounds are given in Supporting Information Table S1). The screening set consisted of previously reported ARCs or their analogues<sup>20,21,23–25</sup> comprising different ATP-site-targeting fragments; structural variations also included different chirality and number of amino acid residues in the peptidic fragment and linker, incorporation of a chiral spacer, and attachment of a fatty acid moiety. The schematic structures of compounds and the assay results are given in Table 2.

The data revealed that the affinity of compounds toward Haspin strongly depended on the number of Arg residues in the peptidic fragment of conjugates. In general, the addition of two Arg residues led to the increase in affinity of up to 2 orders of magnitude (e.g., series ARC-1034 → ARC-582 → ARC-902; subsequently, this trend came to plateau and no significant difference was observed between ARC-902 versus ARC-1090 or ARC-1197). In the peptidic fragment of the compounds, DArg was preferred over the L-isomer (ARC-902 versus ARC-341);

however, the chirality of the spacer within the elongated linker structure did not affect the affinity of conjugates toward Haspin (ARC-1012 versus ARC-1038). The latter observation was different from the previously reported studies with PKAc (where D-amino acid following the first linker was crucial for high affinity of compounds),<sup>21</sup> and can be attributed to the fact that conjugates with short peptidic part are overall unsuitable for Haspin. The introduction of a myristoyl group (Myr) resulted in the decrease in affinity of conjugates (e.g., ARC-685 versus ARC-684), which could probably be attributed to the fact that incorporation of Myr into the side-chain of lysine deprives the latter of the positive charge of the primary amino group.

In compounds containing Adc as the ATP-site-targeting fragment and six Arg residues as the peptide-targeting fragment, elongation of the linker together with introduction of the chiral spacer increased the affinity of the conjugates 10-fold (ARC-1041 versus ARC-902), similarly to our previous studies with PKAc.<sup>21</sup> In analogous compounds containing 5-(2-amino-pyrimidin-4-yl)-thiophene-2-carboxylic acid moiety (AMTH), however, such a structural modification did not result in the gain of affinity (ARC-668 versus ARC-1141). The importance of flexibility and the length of linker for binding of ARCs to Haspin was illustrated by the series of compounds containing Hidaka's inhibitor H9 moiety, where ARC-903 had an over 20-fold greater affinity than ARC-3010 incorporating a more rigid and shorter linker. Surprisingly, the structure of the ATP-site-targeting aromatic fragment itself did not have a significant impact on the affinity of conjugates toward Haspin; Adc, a nucleoside mimic derived from adenosine, was somewhat preferred over planar nonchiral aromatic systems such as AMTH or H9 (ARC-902 versus ARC-668, ARC-903).

Overall, the results implied that binding of ARCs to basophilic Haspin was strongly driven by positively charged oligoarginine peptide. While the aromatic nucleoside mimics together with linker contained in the ARC structure could affect the ways to bind oligoarginine via restricting or retaining conformational versatility of the complex, their effect on binding energy was not as crucial as that of the number of Arg moieties. Importantly, however, DArg<sub>6</sub> peptide on its own (i.e., without conjugation to nucleoside mimics) was not able to fully

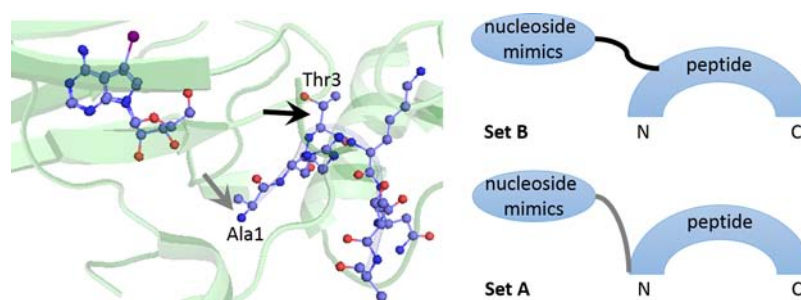


**Figure 2.** Principles of linkage of nucleoside mimics and histone H3(1–7) peptide within the structure of novel conjugates. Left, cocrystal of Haspin with histone H3(1–7) and 5-iodotubercidin (PDB 4OUC). PK is depicted as a green cartoon, histone H3(1–7) and 5-iodotubercidin as colored ball-and-stick structures. The arrows point to the two possible positions in the structure of histone H3(1–7) where the nucleoside mimics of ARCs could be linked. Right, simplified scheme of linkage in compounds belonging to set A or set B.

**Table 4.** Values of the Dissociation Constant  $K_D$  and Selectivity Index of Novel Conjugates (Set A) Established in the Displacement Assays with Haspin and PKAc

nr	schematic structure	$K_D$ , nM <sup>a</sup> Haspin	$K_D$ , nM <sup>a</sup> PKAc	selectivity index <sup>b</sup>
ARC-1141	AMTH-Ahx-DAla-DArg <sub>6</sub> -DLys-Gly	16 (3)	0.06 (0.02)	0.004
1	AMTH-Gly-[Ac-DLys <sup>c</sup> -LArg-LThr-LLys-LGln-LThr-LAla-NH <sub>2</sub> ]	over 15000	over 15000	NC
2	AMTH-Gly-[Ac-DArg <sub>6</sub> -DLys <sup>c</sup> -LArg-LThr-LLys-LGln-LThr-LAla-NH <sub>2</sub> ]	130 (20)	89 (6)	0.7
3	AMTH-Gly-[Ac-LArg <sub>6</sub> -DLys <sup>c</sup> -LArg-LThr-LLys-LGln-LThr-LAla-NH <sub>2</sub> ]	82 (10)	39 (3)	0.5
4	AMTH-Gly-[DLys <sup>c</sup> -LArg-LThr-LLys-LGln-LThr-LAla-NH <sub>2</sub> ]	8800 (1000)	5800 (600)	0.7
5	AMTH-Abu-[DLys <sup>c</sup> -LArg-LThr-LLys-LGln-LThr-LAla-NH <sub>2</sub> ]	13000 (2000)	5000 (500)	0.4
6	AMTH-Abu-[DLys <sup>c</sup> -LArg-LThr-LLys-LGln-LThr-LAla-DArg <sub>6</sub> -NH <sub>2</sub> ]	120 (10)	570 (40)	5
7	AMTH-Abu-[DLys <sup>c</sup> -LArg-LThr-LLys-LGln-LThr-LAla-LArg <sub>6</sub> -NH <sub>2</sub> ]	150 (10)	550 (40)	4
8	AMTH-Ahx-[DDAP-LArg-LThr-LLys-LGln-LThr-LAla-NH <sub>2</sub> ]	5200 (700)	330 (20)	0.06
9	AMTH-Aoc-[DDAP-LArg-LThr-LLys-LGln-LThr-LAla-NH <sub>2</sub> ]	over 15000	51 (3)	below 0.004
10	AMTH-DPro-Gly-[DDAP-LArg-LThr-LLys-LGln-LThr-LAla-NH <sub>2</sub> ]	over 15000	over 15000	NC
11	AMTH-LPro-Gly-[DDAP-LArg-LThr-LLys-LGln-LThr-LAla-NH <sub>2</sub> ]	over 15000	over 15000	NC
12	AMTH-Inp-Gly-[DDAP-LArg-LThr-LLys-LGln-LThr-LAla-NH <sub>2</sub> ]	9500 (1300)	3800 (200)	0.4
13	AMTH-Tnx-Gly-[DDAP-LArg-LThr-LLys-LGln-LThr-LAla-NH <sub>2</sub> ]	over 15000	over 15000	NC

<sup>a</sup>Standard error values are given in brackets ( $N = 2$  or more). <sup>b</sup>For each compound, selectivity index was calculated as the ratio of  $K_D$  values for PKAc and Haspin. For Compounds 1–13, the peptidic fragment corresponding to the modified histone H3(1–7) sequence is shown in square brackets. NC, not calculated. <sup>c</sup>Indicates attachment of the notified fragment to the side-chain of the amino acid.

displace the fluorescent probe from its complex with the kinase even at the highest concentration tested; the same applied to the compound containing only Adc and a linker (ARC-1010). Therefore, it was demonstrated that in order to obtain the considerable affinity of compounds toward Haspin, the linking of a peptidic fragment with a nucleosidic moiety was still required.

**Thermal Shift Assay Using Previously Reported ARC-Scaffolds.** For additional characterization of most of the aforementioned inhibitors, the thermal shift assay that measures the stabilization of a PK upon binding to the compounds<sup>26</sup> was also used (Table 3). The assay was performed with Haspin and three reference PKs, CLK1, CLK2, and DYRK2, which have been reported in the literature as off-targets for the otherwise Haspin-selective inhibitors 5-iodotubercidin and LDN-192960.<sup>10,13</sup>

In the case of measurements with Haspin, the results of displacement assay and thermal shift assay correlated well (i.e., the larger  $\Delta T_m$  values corresponded to lower  $IC_{50}$  values reflecting higher affinity) with the exception of compounds ARC-685 and ARC-3010 whose  $\Delta T_m$  values were smaller than expected for potent inhibitors. Out of 15 screened compounds, 7 resulted in  $\Delta T_m$  values of over 5 °C (according to the literature,  $\Delta T_m$  values over 5 °C typically indicate inhibitors with nM potency),<sup>10</sup> whereas all these compounds contained Arg<sub>6</sub> motif.

The  $\Delta T_m$  values in experiments with reference PKs were remarkably lower (especially in the case of DYRK2), indicating that most of the screened bisubstrate-analogue conjugates possessed selectivity profiles that differed from those of the previously reported ATP site-targeting compounds. While Haspin had highest affinity toward compounds containing an arginine-rich peptide, other PKs had chosen their binders rather according to the ATP-site-targeting fragment, with higher preference toward compounds incorporating AMTH, PIPY, and TIBI. Overall, the results of the temperature shift assay gave us additional confirmation that the development of Haspin-selective inhibitors based on bisubstrate-analogue structural scaffolds is feasible.

**Design and Biochemical Characterization of Novel Compounds.** Next, aiming to increase the selectivity of compounds toward Haspin, we proceeded to design novel Haspin-targeting conjugates comprising a histone H3(1–7) peptide. Based on the established structure–affinity relationship and on synthetic rationale, we chose Adc and AMTH as the ATP-site targeting fragments. In addition, from the 3D-structure of the available Haspin:histone H3(1–7) cocrystal, we predicted two positions in the structure of histone H3(1–7) where nucleoside mimics of ARCs could be linked to (Figure 2): the proximity of the N-terminus of peptide (A), and the proximity of the phosphorylatable residue Thr3 (B). Overall, this approach resulted in generation of two sets of novel



**Table 5.** Values of the Dissociation Constant  $K_D$  and Selectivity Index of Novel Conjugates (Set B) Established in the Displacement Assays with Haspin and PKAc

nr	schematic structure	$K_D$ , nM <sup>a</sup> Haspin	$K_D$ , nM <sup>a</sup> PKAc	selectivity index <sup>b</sup>
ARC-902	Adc-Ahx-DArg <sub>6</sub> -NH <sub>2</sub>	2.6 (0.3)	2.7 (0.4)	1
-	5-iodotubercidin	3.9 (0.4)	over 15000	over 4000
14	Adc-Ahx-DLys <sup>c</sup> [Ac-LAla-LArg-LAsp <sup>c</sup> -Llys-LGln-LAla-LAla-NH <sub>2</sub> ]-NH <sub>2</sub>	5200 (700)	1700 (100)	0.3
15	Adc-Ahx-DAsp <sup>c</sup> [LAla-LArg-Llys <sup>c</sup> -Llys-LGln-LThr-LAla-NH <sub>2</sub> ]-NH <sub>2</sub>	170 (40)	1600 (300)	9
16	Adc-Ahx-DAsp <sup>c</sup> [LAla-LArg-Llys <sup>c</sup> -Llys-LGln-LThr-LAla-NH <sub>2</sub> ]-OH	150 (19)	7700 (1400)	50
17	Adc-Ahx-DAsp <sup>c</sup> [LAla-LArg-Llys <sup>c</sup> -Llys-LGln-LThr-LAla-DLys(Myr)-NH <sub>2</sub> ]-OH	100 (4)	190 (27)	2
18	Adc-Ahx-DAsp <sup>c</sup> [LAla-LArg-Llys <sup>c</sup> -Llys-LGln-LThr-LAla-LArg <sub>6</sub> -NH <sub>2</sub> ]-NH <sub>2</sub>	0.42 (0.14)	38 (4)	90
19	Adc-Ahx-DAsp <sup>c</sup> [LAla-LArg-Llys <sup>c</sup> -Llys-LGln-LThr-LAla-DArg <sub>6</sub> -NH <sub>2</sub> ]-NH <sub>2</sub>	0.88 (0.15)	27 (3)	30
20	Adc-Ahx-Abu-[LAla-LArg-Llys <sup>c</sup> -Llys-LGln-LThr-LAla-NH <sub>2</sub> ]	over 15000	5300 (1000)	below 0.4
21	AMTH-Ahx-Abu-[LAla-LArg-Llys <sup>c</sup> -Llys-LGln-LThr-LAla-NH <sub>2</sub> ]	over 15000	1600 (700)	below 0.1
22	Adc-Ahx-DAsp <sup>c</sup> [LArg <sub>6</sub> -LAla-LArg-Llys <sup>c</sup> -Llys-LGln-LThr-LAla-NH <sub>2</sub> ]-NH <sub>2</sub>	23 (4)	2.9 (0.6)	0.1
23	Adc-Ahx-DAsp <sup>c</sup> [DArg <sub>6</sub> -LAla-LArg-Llys <sup>c</sup> -Llys-LGln-LThr-LAla-NH <sub>2</sub> ]-NH <sub>2</sub>	14 (2)	17 (2)	1
24	Adc-Ahx-DAsp-NH <sub>2</sub>	over 15000	over 15000	NC
25	LAla-LArg-Llys-Llys-LGln-LThr-LAla-DArg <sub>6</sub> -NH <sub>2</sub>	5800 (1800)	over 15000	over 3

<sup>a</sup>Standard error values are given in brackets ( $N = 2$  or more). <sup>b</sup>For each compound, selectivity index was calculated as the ratio of  $K_D$  values for PKAc and Haspin. For Compounds 14–23, the peptidic fragment corresponding to the modified histone H3(1–7) sequence is shown in square brackets. NC, not calculated. <sup>c</sup>Indicates attachment of the notified fragment to the side-chain of the amino acid.

compounds (detailed structures of compounds are given in Supporting Information Table S1).

The affinities of both sets of novel compounds were characterized in displacement assay with Haspin and the fluorescent probe ARC-1081. In order to establish whether the novel compounds were potentially selective toward Haspin, the displacement assay was also performed with a basophilic reference PK, the catalytic subunit of cAMP-dependent protein kinase (PKAc). The determined affinities of the new compounds are presented in Table 4 and Table 5; some representative displacement curves are shown in Supporting Information Figure S1. Importantly, the dissociation constant  $K_D$  value calculated from the displacement  $IC_{50}$  value for reference compound 5-iodotubercidin in assay with Haspin was very comparable to the inhibitory potency of the compound ( $IC_{50}$  value of 3–9 nM reported for inhibition assay performed at ATP concentration close to  $K_M$ ).<sup>9,10</sup> The  $K_D$  value for starting compound ARC-902 in assay with PKAc was also in very good agreement with the previously published data (inhibition constant  $K_i$  value of 3.2 nM).<sup>23</sup>

**Set A: Linkage via N-Terminal Region of Histone H3(1–7) (Compounds 1–13).** The compounds of set A contained AMTH as the ATP-site targeting fragment and had amidated C-termini (Table 5). Amidation was necessary for both the synthetic rationale and improvement of affinity of the conjugates as it masked the negative charge of the C-terminal carboxylate. In Compounds 1–7, Ala1 of histone H3(1–7) was replaced with D-Lys (the side-chain of Ala1 in the PDB 4OUC cocrystal was pointing away from the ATP-site; thus, the change of chirality L → D was expected to “flip” the position of this side-chain) that was then connected via its side-chain to the linker and AMTH moiety. In Compounds 8–13, Ala1 was replaced with D-diaminopropionic acid moiety (D-Dap) that was then connected via its N-terminus to the linker and nucleosidic moiety. The structural variations in the compound set also included acylation of N-terminus of histone H3(1–7)-like peptide, and incorporation of different linkers between the nucleosidic moiety and peptidic fragment. Additionally, the Arg<sub>6</sub> motif (L or D) was added in some cases to the N- or C-terminus of histone H3(1–7)-like peptide, in order to investigate how incorporation of both the selective peptide

and the relatively promiscuous oligoarginine sequence can influence the selectivity of conjugates to Haspin versus PKAc. It was also presumed that oligoarginine as a cell plasma membrane-penetrative peptide sequence<sup>27</sup> could facilitate internalization of developed compounds into live cells in future studies.

All compounds in set A possessed lower affinity toward Haspin than the reference compound ARC-1141; on the other hand, as compared to ARC-1141, the selectivity toward Haspin versus PKAc for all conjugates of set A (except Compound 9) was improved by 1 to 3 orders of magnitude. The latter result indicated that incorporation of Haspin-selective peptide into the structure biased the selectivity profile of conjugates toward Haspin. The acylation of the N-terminus of histone H3(1–7)-like peptide caused 2-fold drop of affinity of conjugates toward Haspin (Compound 1 versus Compound 4), which might be explained by disruption of hydrogen bond developed between N-terminal Ala of histone H3(1–7) and Glu613 of Haspin (according to cocrystal PDB 4OUC). Another reason could be masking of a positive charge of the free amino group at the N-terminus of peptide that was important for binding to basophilic PKs (which would also explain over 2-fold reduction of affinity of the acylated compound toward PKAc).





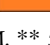
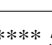
The incorporation of the Arg<sub>6</sub> motif resulted in the dramatic increase of affinity of conjugates toward Haspin as well as PKAc (e.g., Compound 2 versus Compound 1). The comparison of selectivity indices of Compounds 6 and 7 versus Compounds 2 and 3 showed that the positioning of the Arg<sub>6</sub> motif relative to the N- versus C-terminus of histone H3(1–7)-like peptide served as selectivity determinant: N-terminal Arg<sub>6</sub> was preferred by PKAc, whereas C-terminal Arg<sub>6</sub> was preferred by Haspin. Importantly, this observation goes in line with the previously reported preference of Haspin to phosphorylate the residues positioned close to the N-terminus of protein substrates<sup>28</sup> indicating that attachment of longer sequences to the N-terminus of phosphorylatable residue disrupts the recognition of substrate by Haspin.

Of the compounds without the Arg<sub>6</sub> motif, the best affinity toward Haspin was revealed by Compound 8 ( $K_D$  value of 5200 nM). However, Compounds 8 and 9, that both shared the same structural scaffold where the AMTH moiety was linked directly

Table 6. PK Inhibition Profiles for Compounds 15 and 18 (Established on Commercial Basis by Carina Biosciences within This Study) and Reference Compound ARC-902 (Reported Previously)<sup>23a</sup>

PK	PK Group	Compound 15 5 $\mu$ M	Compound 18 1 $\mu$ M	ARC-902 1 $\mu$ M
HER2	TK	-8	-60	-
AKT1 (PKB $\alpha$ )	AGC	46	97	98**
AKT3 (PKB $\gamma$ )	AGC	28	94	-
AurA	other	-19	48	-
AurB	other	-8	87	-3***
AurC	other	-93	23	-
BRAF	TKL	34*	86*	-
BRSK2 (SAD-A)	CAMK	24	57	-
CDC2 (Cdk1)/CycB1	CMGC	7	99	-
CDC7/ASK	other	-18	-146	-
CDK2/CycA2	CMGC	15	98	12***
CDK2/CycE1	CMGC	-2	88	-
CDK3/CycE1	CMGC	0	74	-
CDK4/CycD3	CMGC	-7	72	-
CDK6/CycD3	CMGC	3	67	-
CDK7/CycH/MAT1	CMGC	-4	-73	-
CDK9/CycT1	CMGC	-1	23	-
CHK1	CAMK	61	102	84***
CHK2	CAMK	46	96	86***
CK2 $\alpha$ 1/ $\beta$	other	-5	-19	-4**
CK2 $\alpha$ 2/ $\beta$	other	-12	-27	-
CLK1	CMGC	58	102	-
COT (MAP3K8)	STE	38*	-38*	-
GSK3 $\beta$	CMGC	-3	-11	44**
Haspin	other	102	99	-
LATS2	AGC	58	102	-
MSK1	AGC	55	101	98***
NEK1	other	8	84	-
NEK2	other	4	-23	18****
NEK6	other	2	61	6****
NEK7	other	-2	37	42***
NEK9	other	15	65	-
p38 $\alpha$ (MAPK14)	other	2	33	21****
p70S6K	AGC	61	100	93***
PIM1	CAMK	73	102	-
PIM2	CAMK	59	102	62**
PKA $\alpha$	AGC	98	100	89***
PKC $\alpha$	AGC	51	100	69***
PLK1	other	-9	-84	19**
PLK2	other	7	-56	-
ROCK2	AGC	96	102	100***
RSK1	AGC	11	95	72****
SGK	AGC	11	99	84***

Colour code:					
Colour	% inhibition	Colour	% inhibition	Colour	% inhibition
	below 20		40-60		above 80
	20-40		60-80		no data

<sup>a</sup>Final total concentrations of ATP in the assay. \* 1 mM. \*\* 5  $\mu$ M. \*\*\* 20  $\mu$ M. \*\*\*\* 50  $\mu$ M; no asterisk, close to  $K_m$ (ATP) value for a given PK.

to the N-terminal part of the histone H3(1–7)-like peptide, displayed even higher affinity toward PKAc than toward Haspin. Interestingly, the introduction of rigid cycles into the linker structure of this ARC-scaffold caused a sharp drop of affinity of conjugates toward both PKs (Compounds 10–13 versus Compound 8). Indeed, the previously reported cocrystal structures of ARCs with PKAc indicated that connection of an aromatic moiety of ARC via a flexible linker to the N-terminus of a basic D-amino acid (i.e., first amino acid of the peptidic fragment of conjugate) was optimal for binding of the resulting conjugate to PKAc.<sup>21</sup> Namely, such “architecture” enabled bending of the rest of the positively charged peptidic fragment of ARC toward the interaction-forming amino acid residues in PKAc serving as the hot-spots of substrate recognition (such as Glu127, Glu170, Glu203, and Glu230).<sup>29</sup> The different pattern of substrate binding in Haspin and the previous notion that Haspin could be sensitive to modifications at the N-terminus of

the substrate sequence go hence in line with the structure–affinity relationship observed here.

**Set B: Linkage via Phosphorylatable Region of Histone H3(1–7) (Compounds 14–23).** Most of the novel compounds of set B contained Adc as the ATP-site targeting fragment; in Compound 21, AMTH was substituted for Adc (Table 5). Similarly to set A, all compounds of the set B had amidated C-termini. In Compound 14, Thr3 was replaced with LAsp that was then connected via its side-chain to the side-chain of chiral spacer (DLys), preceded by linker and nucleosidic moiety (for synthetic reasons, in Compound 14 the N-terminus of histone H3(1–7)-like peptide was acylated, and Thr6 of histone H3(1–7) was replaced with LAla). In Compounds 15–23, Thr3 was replaced with LLys that was then connected via its side-chain to the side-chain of chiral spacer (DAsp; Compounds 15–19 and 22–23) or directly to the linker (Compounds 20–21), preceded by nucleosidic moiety. Analogously to set A, the

further structural variations in set B included incorporation of different linkers between the nucleosidic moiety and the peptidic part, and addition of Arg<sub>6</sub> motif (L or D) to the N- or C-terminus of the histone H3(1–7)-like peptide.

Despite the fact that in set B the gain in selectivity of compounds as compared to the selectivity index of the reference compound ARC-902 was not strikingly pronounced; over 8-fold higher affinities toward Haspin than toward PKAc could be achieved for most efficient conjugates (Compounds 15, 16, 18, and 19). Overall, the novel conjugates of set B confirmed the trends of the structure–affinity relationship established for set A. Acylation of the N-terminus of the histone H3(1–7)-like peptide caused a 30-fold drop of affinity toward Haspin (Compound 14 versus Compound 15). Importantly, it was demonstrated that chiral spacer (D-amino acid) was required for correct positioning of the fragments of conjugate to their binding sites in Haspin (and to smaller extent in PKAc), as replacement of the chiral spacer with a nonchiral chain of approximately the same length resulted in the sharp decrease of affinity of compounds (Compound 20 versus Compound 15). This goes in line with the aforementioned notion that, while long flexible linker structures might generally be profitable for bisubstrate inhibitors,<sup>30</sup> a chiral spacer following the nucleosidic moiety and linker of conjugate could be required for directing the peptidic part of the conjugate toward the substrate-binding site and not toward solution.<sup>21</sup>

Compounds 15–17 possessed  $K_D$  values of 100–170 nM, which was the best result for all novel compounds not incorporating oligoarginine. Moreover, Compound 16 demonstrated 50-fold selectivity toward Haspin versus PKAc, which could be attributed to the introduction of free carboxylate instead of amide to the C-terminus of the chiral spacer: this modification was well tolerated by Haspin, but not by PKAc. From the previously reported cocrystals of ARCs with PKAc,<sup>21,29</sup> it was evident that in several cases, the amide group at the C-terminus of the chiral spacer was involved in formation of hydrogen bonds with the Gly-rich loop of the kinase; these interactions might therefore be crucial for the optimal positioning of ARC in complex with PKAc, but not Haspin. On the other hand, the introduction of Myr to the C-terminal part of the histone H3(1–7)-like peptide caused a slight improvement of the affinity of the resulting conjugate toward Haspin, but a 40-fold increase in its affinity toward PKAc (Compound 17 versus Compound 16). The latter result could probably be explained by interaction of the Myr chain with the hydrophobic pocket of PKAc often referred to as the (P+1)-pocket.<sup>31</sup>

The introduction of the Arg<sub>6</sub> motif into the structure of compounds resulted again in the dramatic increase of their affinity toward both PKs, and subnanomolar  $K_D$  values could be achieved for Compounds 18 and 19 toward Haspin (showing thus higher affinity than 5-iodotubercidin). Importantly, the affinity of Compound 18 was 90-fold higher and the affinity of Compound 19 was 30-fold higher toward Haspin than toward PKAc; again, the positioning of Arg<sub>6</sub> motif at the C-terminus (not N-terminus) of histone H3(1–7)-like peptide was crucial for achieving selectivity. The fluorescent probe ARC-3379 (see structure in Supporting Information) derived from Compound 19 also possessed 20-fold selectivity toward Haspin versus PKAc, and could be successfully displaced from its complex with Haspin by both ATP site-targeting compound 5-

iodotubercidin as well as the peptidic Compound 25 (Supporting Information Figure S2).

Finally, it was confirmed that neither the peptidic part of the conjugates (Compound 25) nor the fragment binding to ATP-site (Compound 24) possessed significant affinity toward Haspin. According to the ARC-1081 displacement data presented in Table 5, the increase of affinity upon conjugation of the peptidic part via the linkers and chiral spacer with the nucleosidic moiety was over 6000-fold (Compound 19 versus Compound 25). The latter facts hence pointed indirectly to the bisubstrate character of the most effective novel conjugates (i.e., simultaneous association with both substrate-binding sites of Haspin).

**Selectivity Profiling and Inhibition Studies of Novel Compounds.** Eventually, wide selectivity testing of two novel conjugates was performed toward a panel of 43 kinases. Compounds 15 (final total concentration in the assay of 5  $\mu$ M) and 18 (final total concentration in the assay of 1  $\mu$ M) were profiled on the commercial basis at Carina Biosciences using inhibition assays (IMAP assay or Off-Chip Mobility Shift Assay). The established inhibition percentages (Table 6) were compared to those obtained for the reference compound ARC-902 (final total concentration in the assay of 1  $\mu$ M) in the previous studies (performed on the commercial basis at the Division of Signal Transduction Therapy, University of Dundee).<sup>23</sup>

The list of targets chosen for profiling included PKs serving as important players in mitosis (e.g., Aurora, CDK, NEK families) as well as several other PKs (e.g., basophilic Akt, Pim, ROCK families) that had previously been included in the selectivity profiling within the frame of our previous studies. Tyrosine kinase HER2 and acidophilic Ser/Thr PK CK2 were included as the presumable negative controls. As the profiling of Compounds 15 and 18 was performed at relatively high concentrations of the compounds (i.e., compared to their affinities established the displacement assay), it was expected that novel conjugates will inhibit several PKs of the chosen set.

Indeed, Compound 18 inhibited at 1  $\mu$ M concentration efficiently (i.e., to the extent of 80% or more) most of the basophilic PKs in the panel (including PKs from AGC and CAMK groups, Aurora B and CLK1) with the exception of Auroras A and C and BRSK2. In addition, Compound 18 inhibited several PKs of CDK family (except CDK7 and CDK9) and NEK family (except NEK2 and NEK7). In general, the selectivity profile revealed by Compound 18 was closely similar to that of the reference compound ARC-902, whereas PKs Aurora B, CDK2/CycA, NEK6, Pim2, and PKC $\alpha$  were even more inhibited by Compound 18 than by ARC-902. Expectedly, acidophilic PKs CDC7, CK2, and the PLK family were not inhibited (negative inhibition % values result most likely from the fact that peptide-containing conjugates might serve as reagents reducing the nonspecific binding of PKs to the surfaces, and not from activation of the PKs by conjugates). These results showed that the strong positive charge of the Arg<sub>6</sub> motif made the conjugate “appealing” overall for basophilic PKs irrespective of other amino acids included in the specific peptidic fragment of the inhibitor. This is an important finding given the fact that oligoarginine has frequently been used as the cell plasma membrane-penetrating sequence for intracellular transportation of a variety of “cargoes”; in light of our study, it should be considered that at high concentrations, the oligoarginine moiety could in fact have a profound effect on the selectivity profile of its “cargo”.



Compound **15**, on the other hand, possessed a remarkably more focused selectivity profile even at 5  $\mu\text{M}$  concentration (higher concentration was chosen for screening as Compound **15** had lower affinity toward Haspin in displacement assay than Compound **18**). Out of 43 PKs, only 3 were inhibited over 80% (Haspin, PKAc, and ROCK2); another 3 PKs were inhibited to the extent of 60–80% relative to noninhibited control (CHK1, p70S6K, and Pim1). These results indicated that Compound **15** served as a successful example of Haspin-targeting bisubstrate-analogue inhibitors, which not only profited in the aspect of affinity toward Haspin (i.e., from linking of two otherwise weakly binding fragments, Adc and histone H3(1–7)-like peptide), but also retained Haspin-selectivity conferred by the peptidic fragment derived from the natural protein substrate. This is a remarkable achievement given the reported evidence that conjugation of a target-specific peptide with an additional moiety does not always translate into the conservation of selective properties of the initial fragment(s).<sup>32</sup>

Finally, we examined the physiological effect of 5 novel conjugates (Compounds **15**–**19**) and a reference compound 5-iodotubercidin on the Haspin pathways in nocodazole-synchronized live HeLa cells by monitoring decrease in the phosphorylation of Thr3 of histone H3 upon 20 h incubation with 5  $\mu\text{M}$  compounds. A relatively high concentration of compounds was chosen, as we had previously seen that internalization of ARCs into the cells is the factor limiting their applicability for the *in vitro* experiments, but it can be significantly improved at concentrations of compounds above 1  $\mu\text{M}$ .<sup>18,33</sup> Of tested conjugates, Compound **18** caused 33% decrease of phosphorylation of histone H3; in a control experiment with the same concentration of 5-iodotubercidin, a 95% decrease of phosphorylation was observed (Supporting Information Figure S3). Similar tendencies were observed in the case of 1 h incubation with 5  $\mu\text{M}$  compounds (data not shown). Overall, these results indicated that while the biochemical potency of the novel conjugates might be better than that of the 5-iodotubercidin, the cell plasma membrane-penetrative properties should be improved. The incorporation of Arg<sub>6</sub> motif or Myr may not be sufficient for successful internalization of ARCs into live cells, and the less Haspin-targeted selectivity profile of the Compounds **17**–**19** could also diminish their physiological effects due to the presence of a variety of mitotic PKs more abundant than Haspin. Therefore, our aim in future studies will be the development of cell plasma membrane-penetrative probes with focused Haspin-selectivity profile using Compounds **15** and **16** as the lead scaffolds.

## CONCLUSION

In this work, we performed wide screening of nucleoside mimic–peptide conjugates toward the mitotic protein kinase Haspin. In total, the affinity of 51 compounds toward Haspin and a basophilic reference kinase PKAc was evaluated including 7 fluorescent probes and 26 novel compounds comprising peptides derived from the only known physiological substrate of Haspin, histone H3. The structure–affinity relationship demonstrated that Haspin was extremely sensitive to modifications at the N-terminal amino acid residue of histone H3(1–7)-like peptide. The novel conjugate with the highest affinity (Compound **18**) possessed a subnanomolar  $K_D$  value toward Haspin and revealed 90-fold higher affinity toward Haspin than toward the basophilic reference kinase, PKAc. The profiling of two novel conjugates at elevated concentrations (1  $\mu\text{M}$  and 5  $\mu\text{M}$ ) toward a panel of 43 PKs (including the most

important players in mitosis) indicated that a conjugate incorporating a short peptide with Haspin substrate-like sequence from the N-terminus of histone H3 possessed higher Haspin selectivity than its oligoarginine-containing counterpart. Moreover, incorporation of both the histone H3-like peptide and oligoarginine resulted in the loss of Haspin selectivity. Overall, the novel scaffolds generated in this work as well as the established structure–affinity and structure–selectivity relationship will strongly contribute to development of Haspin-targeting selective high-affinity probes.

## EXPERIMENTAL PROCEDURES

**Materials.** Chemicals and resins for synthesis were obtained from Iris Biotech, Neosystem, Novabiochem, Caslo, Advanced ChemTech, or AnaSpec. 5-Iodotubercidin was from Cayman Chemicals. PKAc type  $\alpha$  (recombinant human protein, full sequence) was a kind gift from Prof. Richard A. Engh (Norwegian Structural Biology Centre, University of Tromsø).

**Synthesis of Conjugates.** The novel conjugates were synthesized according to solid-phase peptide synthesis procedures using the previously published protocols.<sup>20</sup> After synthesis, the compounds were purified with Shimadzu LC Solution HPLC system (Prominence) using a Gemini C18 reverse-phase column (5  $\mu\text{m}$ , 25 cm  $\times$  0.46 cm), manual injection, and a diode array UV–vis detector (SPD M20A). The high-resolution mass spectra (HRMS) of compounds were measured with Thermo Electron LTQ Orbitrap mass spectrometer. A NanoDrop 2000c (Thermo Scientific) spectrophotometer was used for quantification of the compounds based on the following molar extinction coefficient ( $\epsilon$ ) values: Adc (15 000  $\text{M}^{-1} \text{cm}^{-1}$  at 260 nm), AMTH (15 000  $\text{M}^{-1} \text{cm}^{-1}$  at 340 nm), H9 (4400  $\text{M}^{-1} \text{cm}^{-1}$  at 323 nm), PIPY (16 000  $\text{M}^{-1} \text{cm}^{-1}$  at 286 nm), PYB (16 900  $\text{M}^{-1} \text{cm}^{-1}$  at 250 nm), TIBI (10 300  $\text{M}^{-1} \text{cm}^{-1}$  at 300 nm), Cy3B (130 000  $\text{M}^{-1} \text{cm}^{-1}$  at 558 nm), or TAMRA (80 000  $\text{M}^{-1} \text{cm}^{-1}$  at 558 nm). The  $\epsilon$  values for DArg<sub>9</sub>-NH<sub>2</sub> peptide and Compound **25** were calculated according to the literature<sup>34</sup> as 9200  $\text{M}^{-1} \text{cm}^{-1}$  and 12 900  $\text{M}^{-1} \text{cm}^{-1}$  at 214 nm, respectively. The detailed synthetic procedures as well as mass spectrometry and HPLC data are presented in the Supporting Information (Supplementary Methods, Table S3 and Table S4).

**Haspin Production and Purification.** Human recombinant Haspin protein (residues 470–798) with a TEV-cleavable N-terminal His<sub>6</sub>-tag was produced and purified according to the previously published protocols.<sup>2</sup> The experimental  $m/z$  of the protein was confirmed by LC-MS using Agilent LC/MSD TOF system.

**Biochemical Assays with Detection of Fluorescence Polarization/Anisotropy.** The fluorescence anisotropy measurements were performed according to the previously published protocols<sup>19</sup> by using PHERAstar microplate reader (BMG Labtech) with an optic module for TAMRA-labeled compounds [ex. 540(20) nm, em. 590(20) and 590(20) nm]. All the solutions of samples were prepared in 384-well low-binding surface microtiter plates (Corning, code 3676). The assay buffer contained 50 mM Hepes (pH 7.5), 150 mM NaCl, 5 mM dithiothreitol, and 0.005% Tween-20. GraphPad Prism version 5.0 (GraphPad Software, Inc.) was used for data processing and analysis.

**Thermal Shift Assay.** Thermal shift assay measurements were performed according to the previously published protocols<sup>26</sup> using a real-time PCR instrument (Mx3005p RT-PCR, Stratagene). The final total concentrations of Haspin and



ARCs in the experiments were 2  $\mu$ M and 12.5  $\mu$ M, respectively. The measurements were performed in PCR low-profile microplate wells (ABgene). The temperature scan was run from 25 to 95 °C at 1 °C/min. GraphPad Prism v 6.0 (GraphPad Software, Inc.) and Microsoft Excel v 2007 software were used for data processing and analysis.

## ■ ASSOCIATED CONTENT

### ■ Supporting Information

Synthesis protocols, structures of all compounds used in this study, HRMS and HPLC data for novel compounds, and so forth. This material is available free of charge via the Internet at <http://pubs.acs.org>.

## ■ AUTHOR INFORMATION

### Corresponding Authors

\*E-mail address: stefan.knapp@sgc.ox.ac.uk. Tel/fax: +44 1865 612933.

\*E-mail address: asko.uri@ut.ee. Tel/fax: +372 737 5275.

### Notes

The authors declare no competing financial interest.

## ■ ACKNOWLEDGMENTS

The help of Ramesh Ekambaram, Erki Enkvist, Anton Konovalov, Kersti Nisuma and Birgit Viira in synthesis of ARC compounds is gratefully acknowledged. This work was supported by grants from the Estonian Research Council (PUT0007 and IUT20-17). K.K. received a Kristjan Jaak stipendium from SA Archimedes. A.C. and S.K. are grateful for financial support by the SGC, a registered charity (number 1097737) that receives funds from AbbVie, Bayer Pharma AG, Boehringer Ingelheim, the Canada Foundation for Innovation, Genome Canada, GlaxoSmithKline, Janssen, Lilly Canada, the Novartis Research Foundation, the Ontario Ministry of Economic Development and Innovation, Pfizer, Takeda, and the Wellcome Trust [092809/Z/10/Z].

## ■ ABBREVIATIONS

Abu, 4-aminobutanoic acid moiety; Adc, adenosine-4'-dehydroxymethyl-4'-carboxylic acid moiety; Ahx, 6-aminohexanoic acid moiety; AMSE, 5-(2-aminopyrimidin-4-yl)-selenophene-2-carboxylic acid moiety; AMTH, 5-(2-aminopyrimidin-4-yl)-thiophene-2-carboxylic acid moiety; ARC, adenosine analogue-oligoarginine conjugate; DAP, diaminopropionic acid moiety; H9, N-aminoethyl-5-isoquinolinesulfonamide moiety; Inp, isonipecotic acid (4-piperidinecarboxylic acid) moiety; Myr, myristoyl; PIPY, 4-(piperazin-1-yl)-7H-pyrrolo[2,3-d]pyrimidine moiety; PK, protein kinase; PKAc, catalytic subunit of cAMP-dependent protein kinase; PYB, 3-(pyridin-4-yl)benzoic acid moiety; TIBI, 4,5,6,7-tetraiodo-1H-benzimidazole moiety; Tnx, tranexamic acid (trans-4-(aminomethyl)-cyclohexanecarboxylic acid) moiety

## ■ REFERENCES

- (1) Higgins, J. M. (2001) Haspin-like proteins: a new family of evolutionarily conserved putative eukaryotic protein kinases. *Protein Sci.* 10, 1677–1684.
- (2) Eswaran, J., Patnaik, D., Filippakopoulos, P., Wang, F., Stein, R. L., Murray, J. W., Higgins, J. M., and Knapp, S. (2009) Structure and functional characterization of the atypical human kinase haspin. *Proc. Natl. Acad. Sci. U. S. A.* 106, 20198–20203.
- (3) Villa, F., Capasso, P., Tortorici, M., Forneris, F., de Marco, A., Mattevi, A., and Musacchio, A. (2009) Crystal structure of the catalytic

domain of Haspin, an atypical kinase implicated in chromatin organization. *Proc. Natl. Acad. Sci. U. S. A.* 106, 20204–20209.

- (4) Dai, J., Sultan, S., Taylor, S. S., and Higgins, J. M. (2005) The kinase haspin is required for mitotic histone H3 Thr 3 phosphorylation and normal metaphase chromosome alignment. *Genes Dev.* 19, 472–488.

(5) Yamagishi, Y., Honda, T., Tanno, Y., and Watanabe, Y. (2010) Two histone marks establish the inner centromere and chromosome bi-orientation. *Science* 330, 239–243.

(6) Dodson, C. A., Haq, T., Yeoh, S., Fry, A. M., and Bayliss, R. (2013) The structural mechanisms that underpin mitotic kinase activation. *Biochem. Soc. Trans.* 41, 1037–1041.

(7) Kelly, A. E., Gheno, C., Xue, J. Z., Zierhut, C., Kimura, H., and Funabiki, H. (2010) Survivin reads phosphorylated histone H3 threonine 3 to activate the mitotic kinase Aurora B. *Science* 330, 235–239.

(8) Wang, F., Dai, J., Daum, J. R., Niedzialkowska, E., Banerjee, B., Stukenberg, P. T., Gorbisky, G. J., and Higgins, J. M. (2010) Histone H3 Thr-3 phosphorylation by Haspin positions Aurora B at centromeres in mitosis. *Science* 330, 231–235.

(9) Wang, F., Ulyanova, N. P., Daum, J. R., Patnaik, D., Kateneva, A. V., Gorbisky, G. J., and Higgins, J. M. (2012) Haspin inhibitors reveal centromeric functions of Aurora B in chromosome segregation. *J. Cell Biol.* 199, 251–268.

(10) De Antoni, A., Maffini, S., Knapp, S., Musacchio, A., and Santaguida, S. (2012) A small-molecule inhibitor of Haspin alters the kinetochore functions of Aurora B. *J. Cell Biol.* 199, 269–284.

(11) Maiolica, A., de Medina-Redondo, M., Schoof, E. M., Chaikuad, A., Villa, F., Gatti, M., Jeganathan, S., Lou, H. J., Novy, K., Hauri, S., Toprak, U. H., Herzog, F., Meraldi, P., Penengo, L., Turk, B. E., Knapp, S., Lindig, R., and Aebersold, R. (2014) Modulation of the chromatin phosphoproteome by the haspin protein kinase. *Mol. Cell Proteomics* 13, 1724–1740.

(12) Patnaik, D., Xian, Jun, Glicksman, M. A., Cuny, G. D., Stein, R. L., and Higgins, J. M. (2008) Identification of small molecule inhibitors of the mitotic kinase haspin by high-throughput screening using a homogeneous time-resolved fluorescence resonance energy transfer assay. *J. Biomol. Screen.* 13, 1025–1034.

(13) Cuny, G. D., Robin, M., Ulyanova, N. P., Patnaik, D., Pique, V., Casano, G., Liu, J. F., Lin, X., Xian, J., Glicksman, M. A., Stein, R. L., and Higgins, J. M. (2010) Structure-activity relationship study of acridine analogs as haspin and DYRK2 kinase inhibitors. *Bioorg. Med. Chem. Lett.* 20, 3491–3494.

(14) Uri, A., Lust, M., Vaasa, A., Lavogina, D., Viht, K., and Enkvist, E. (2010) Bisubstrate fluorescent probes and biosensors in binding assays for HTS of protein kinase inhibitors. *Biochim. Biophys. Acta* 1804, 541–546.

(15) Lavogina, D., Enkvist, E., and Uri, A. (2010) Bisubstrate inhibitors of protein kinases: from principle to practical applications. *ChemMedChem* 5, 23–34.

(16) Ekambaram, R., Enkvist, E., Vaasa, A., Kasari, M., Raidaru, G., Knapp, S., and Uri, A. (2013) Selective bisubstrate inhibitors with subnanomolar affinity for protein kinase Pim-1. *ChemMedChem* 8, 909–913.

(17) Lavogina, D., Kalind, K., Bredihhina, J., Hurt, M., Vaasa, A., Kasari, M., Enkvist, E., Raidaru, G., and Uri, A. (2012) Conjugates of 5-isoquinolinesulfonylamides and oligo-D-arginine possess high affinity and selectivity towards Rho kinase (ROCK). *Bioorg. Med. Chem. Lett.* 22, 3425–3430.

(18) Vaasa, A., Lust, M., Terrin, A., Uri, A., and Zaccolo, M. (2010) Small-molecule FRET probes for protein kinase activity monitoring in living cells. *Biochem. Biophys. Res. Commun.* 397, 750–755.

(19) Vaasa, A., Viil, I., Enkvist, E., Viht, K., Raidaru, G., Lavogina, D., and Uri, A. (2009) High-affinity bisubstrate probe for fluorescence anisotropy binding/displacement assays with protein kinases PKA and ROCK. *Anal. Biochem.* 385, 85–93.

(20) Lavogina, D., Nickl, C. K., Enkvist, E., Raidaru, G., Lust, M., Vaasa, A., Uri, A., and Dostmann, W. R. (2010) Adenosine analogue-oligo-arginine conjugates (ARCs) serve as high-affinity inhibitors and

fluorescence probes of type I cGMP-dependent protein kinase (PKGI $\alpha$ ). *Biochim. Biophys. Acta* 1804, 1857–1868.

(21) Lavogina, D., Lust, M., Viil, I., König, N., Raidaru, G., Rogozina, J., Enkvist, E., Uri, A., and Bossemeyer, D. (2009) Structural analysis of ARC-type inhibitor (ARC-1034) binding to protein kinase A catalytic subunit and rational design of bisubstrate analogue inhibitors of basophilic protein kinases. *J. Med. Chem.* 52, 308–321.

(22) Enkvist, E., Vaasa, A., Kasari, M., Kriisa, M., Ivan, T., Ligi, K., Raidaru, G., and Uri, A. (2011) Protein-induced long lifetime luminescence of nonmetal probes. *ACS Chem. Biol.* 6, 1052–1062.

(23) Enkvist, E., Lavogina, D., Raidaru, G., Vaasa, A., Viil, I., Lust, M., Viht, K., and Uri, A. (2006) Conjugation of adenosine and hexa-(D-arginine) leads to a nanomolar bisubstrate-analog inhibitor of basophilic protein kinases. *J. Med. Chem.* 49, 7150–7159.

(24) Räägel, H., Lust, M., Uri, A., and Pooga, M. (2008) Adenosine-oligoarginine conjugate, a novel bisubstrate inhibitor, effectively dissociates the actin cytoskeleton. *FEBS J.* 275, 3608–3624.

(25) Lavogina, D., Budu, A., Enkvist, E., Hopp, C. S., Baker, D. A., Langsley, G., Garcia, C. R., and Uri, A. (2014) Targeting Plasmodium falciparum protein kinases with adenosine analogue-oligoarginine conjugates. *Exp. Parasitol.* 138, 55–62.

(26) Fedorov, O., Niesen, F. H., and Knapp, S. (2012) Kinase inhibitor selectivity profiling using differential scanning fluorimetry. *Methods Mol. Biol.* 795, 109–118.

(27) Futaki, S., Hirose, H., and Nakase, I. (2013) Arginine-rich peptides: methods of translocation through biological membranes. *Curr. Pharm. Des.* 19, 2863–2868.

(28) Kettenbach, A. N., Wang, T., Faherty, B. K., Madden, D. R., Knapp, S., Bailey-Kellogg, C., and Gerber, S. A. (2012) Rapid determination of multiple linear kinase substrate motifs by mass spectrometry. *Chem. Biol.* 19, 608–618.

(29) Pflug, A., Rogozina, J., Lavogina, D., Enkvist, E., Uri, A., Engh, R. A., and Bossemeyer, D. (2010) Diversity of bisubstrate binding modes of adenosine analogue-oligoarginine conjugates in protein kinase a and implications for protein substrate interactions. *J. Mol. Biol.* 403, 66–77.

(30) Kane, R. S. (2010) Thermodynamics of multivalent interactions: influence of the linker. *Langmuir* 26, 8636–8640.

(31) Yang, J., Garrod, S. M., Deal, M. S., Anand, G. S., Woods, V. L., Jr., and Taylor, S. (2005) Allosteric network of cAMP-dependent protein kinase revealed by mutation of Tyr204 in the P+1 loop. *J. Mol. Biol.* 346, 191–201.

(32) Livnah, N., Yechezkel, T., Salitra, Y., Perlmutter, B., Ohne, O., Cohen, I., Litman, P., and Senderowitz, H. (2004) Protein Kinase Inhibitors Comprising ATP Mimetics Conjugated to Peptides or Peptidomimetics. Patent No. EP1416934.

(33) Kriisa, M., Sinijärvi, H., Vaasa, A., Enkvist, E., Kostenko, S., Moens, U., and Uri, A. (2014) Inhibition of CREB phosphorylation by conjugates of adenosine analogues and arginine-rich peptides, inhibitors of PKA catalytic subunit. *ChemBioChem*, DOI: 10.1002/cbic.201402526.

(34) Kuipers, B. J., and Gruppen, H. (2007) Prediction of molar extinction coefficients of proteins and peptides using UV absorption of the constituent amino acids at 214 nm to enable quantitative reverse phase high-performance liquid chromatography-mass spectrometry analysis. *J. Agric. Food Chem.* 55, 5445–5451.